ARTICLES

Journal of Semiconductors
(2019) 40, 052701
doi: 10.1088/1674-4926/40/5/052701

Realizing super-long Cu_2O nanowires arrays for high-efficient water splitting applications with a convenient approach

Nasori Nasori[1, 2], Tianyi Dai[3], Xiaohao Jia[4, 5], Agus Rubiyanto[2], Dawei Cao[3], Shengchun Qu[4, 5], Zhanguo Wang[4, 5], Zhijie Wang[4, 5, †], and Yong Lei[1, †]

[1]Institute of Physics & IMN MacroNano® (ZIK), Ilmenau University of Technology, 98693 Ilmenau, Germany

[2]Physics Department, Faculty of Science, Institute of Technology Sepuluh Nopember, Surabaya, 6200, Indonesia

[3]Department of Physics, Zhenjiang Key Laboratory for Advanced Sensing Materials and Devices, Faculty of Science, Jiangsu University, Zhenjiang 212013, China

[4]Key Laboratory of Semiconductor Materials Science, Beijing Key Laboratory of Low Dimensional Semiconductor Materials and Devices, Institute of Semiconductors, Chinese Academy of Sciences, Beijing 100083, China

[5]Center of Materials Science and Optoelectronics Engineering, University of Chinese Academy of Sciences, Beijing 100049, China

Abstract: Nanowire (NW) structures is an alternative candidate for constructing the next generation photoelectrochemical water splitting system, due to the outstanding optical and electrical properties. NW photoelectrodes comparing to traditional semiconductor photoelectrodes shows the comparatively shorter transfer distance of photo-induced carriers and the increase amount of the surface reaction sites, which is beneficial for lowering the recombination probability of charge carriers and improving their photoelectrochemical (PEC) performances. Here, we demonstrate for the first time that super-long Cu_2O NWs, more than 4.5 μm, with highly efficient water splitting performance, were synthesized using a cost-effective anodic alumina oxide (AAO) template method. In comparison with the photocathode with planar Cu_2O films, the photocathode with Cu_2O NWs demonstrates a significant enhancement in photocurrent, from –1.00 to –2.75 mA/cm^2 at –0.8 V versus Ag/AgCl. After optimization of the photoelectrochemical electrode through depositing Pt NPs with atomic layer deposition (ALD) technology on the Cu_2O NWs, the plateau of photocurrent has been enlarged to –7 mA/cm^2 with the external quantum yield up to 34% at 410 nm. This study suggests that the photoelectrode based on Cu_2O NWs is a hopeful system for establishing high-efficiency water splitting system under visible light.

Key words: super-long nanowires; P-type Cu_2O; AAO template; photoelectrochemical water splitting

Citation: N Nasori, T Y Dai, X H Jia, A Rubiyanto, D W Cao, S C Qu, Z G Wang, Z J Wang, and Y Lei, Realizing super-long Cu_2O nanowires arrays for high-efficient water splitting applications with a convenient approach[J]. *J. Semicond.*, 2019, 40(5), 052701. http://doi.org/10.1088/1674-4926/40/5/052701

1. Introduction

Since Fujishima and Honda initially, in 1972, reported hydrogen generation in a photoelectrochemical water splitting device by introducing the TiO_2 electrode[1]. The conversion from solar energy into chemical fuels like hydrogen is a most practicable method to solve the world-wide sustainable energy challenges. However, as has been discussed often, until now, the reported conversion efficiency is still too low for application in reality[2–10]. To solve this problem, building novel morphologies has been an effective method in fundamentally improving the efficiency of photocatalytic water splitting, based on their structural advantage depending on the size and shape. Nanowire, as a typical nanostructure, has been successfully manufactured in various semiconductors for enhancing the PEC performances, such as TiO_2, ZnO[10].

Cu_2O, as an attractive candidate for light energy conversion, possessing a favorable direct band gap (E_g ~ 2.1 eV), which the maximum photocurrent in theory is of 15 mA/cm^2 and the light-to-H_2 conversion efficiency is 18% under a standard solar radiation[10–14]. Besides, compared to other p-type PEC materials, Cu is much abundant and the preparation method is low-cost by industrial proven. Recently, the Cu_2O thin films photocathode with highly active of was proposed[14], which reached the large photocurrents of ~7.6 mA/cm^2 at 0 V versus RHE and maintained working for one-hour testing time. In our previous work, we reported an efficacious surface modification for Cu_2O photocathodes by trisodium citrate to realize an impressive PEC performance[15]. These results indicate significant feasible of Cu_2O in photocatalysis water splitting. In particular, for efficiency improvement, various Cu_2O nanostructures with high specific surface area and short charge carrier diffusion lengths compared with bulk materials, have been successfully fabricated, including nanorods, nanowires (NWs), nanotubes, nanocubes, and nanospheres[16–19] and different synthesis[20, 21]. However, super-long Cu_2O NW arrays have been not well reported, for PEC water splitting. In this paper, we synthesize successfully super-long Cu_2O NW arrays by the convenient and low-cost anodic alumina oxide (AAO) template technology. In comparison with the photocathode based on Cu_2O films, the super-long Cu_2O NWs photocathode demonstrates a remarkable enhancement in photocurrent, from –1.00 to

Correspondence to: Z J Wang, wangzj@semi.ac.cn; Y Lei, yong.lei@tu-ilmenau.de

Received 15 FEBRUARY 2019; Revised 26 MARCH 2019.

–2.75 mA/cm^2 at –0.8 V versus Ag/AgCl. Since the photoelectrochemical system was optimized by depositing Pt NPs with ALD on the Cu_2O NWs, the plateau photocurrent has been improved to –7.00 mA/cm^2 at –0.8 V versus Ag/AgCl and the external quantum yield (EQY) is up to 34% at 410 nm. The research results of this work offer an inexpensive, naturally resourceful nanowire material element for applications in photoelectrochemical cells.

2. Experimental

2.1. Preparation of Cu_2O NWs and films

Synthesized from high purity Al foils, AAO templates were fabricated with a two-step anodization in oxalic acid (0.3 M) at 40 V during eight-hours anodization time for the first step and one-hour anodization time for the second step[22, 23]. The AAO pores were broadened in H_3PO_4 solution (5 wt%) for 50 min at 30 °C. After that, a 25 nm-thickness layer of gold was deposited with the process of physical vapor deposition (PVD). Subsequently, Ni film layer was synthesized on the surface of AAO template at a current density of 5 mA/cm^2. The Ni plating solution has $NiSO_4$ (0.38 M), $NiCl_2$ (0.12 M), and H_3BO_3 (0.5 M). The AAO template with gold was utilized as the working electrode, while Ni foil was used as the counter electrode. Then, the backside alumina was removed by $CuCl_2$ solution, and the AAO with Ni layer was obtained. Later on, the sample was soaked in H_3PO_4 (5%) for 30 min in 60 °C in order to remove the barrier layer before the deposition of Cu_2O. At the end, Cu_2O NWs were electrodeposited catholically in a copper sulphate bath (0.4 M) which contained 3 M lactic acid. The pH value of the bath was configured to 12 with caution adding 3 M NaOH. Then Cu_2O NWs were synthesized under a steady potential (–0.40 V versus Ag/AgCl) with a standard three-electrode system for a 90 min. By a heating stage with a real-time temperature probe, the bath temperature was set at 45 °C the whole time. After deposition, the AAO skeleton was removed by immersion in sodium hydroxide aqueous solution (0.1 M) aim time 1 hour and long Cu_2O ordered nanowires were hence obtained. As a comparison, Cu_2O thin films directly on FTO/Au was prepared by the same process.

2.2. Fabrication of photocathodes of Cu_2O NWs and films

The strip of conductive Cu tapes was connect to the uncovered FTO and Ni area of the FTO/Au/Cu_2O and Ni/Cu_2O NWs, respectively, in order to extend the conducting circuit. The Cu tapes were later put through the glass tubes, and then waterproofed with the a/b mixed epoxy adhesive. The area of samples was measured by a computer with the help of Photoshop software.

2.3. Measurements of PEC characteristics

The EQY measurement of the sample was obtained under a xenon lamp (150 W) with a grating monochromator from Newport corporation. Photocurrent–potential (*J*–*V*) curves and impedance characteristic were recorded by the high accuracy Bio-Logic potentiostat (SP-200) in sodium sulphate solution (0.1 M). A reference electrode (Ag/AgCl) and a counter electrode (Pt) were utilized during the measurements. As the light source, a standard 300 W xenon lamp (Newport) was used, and the optical intensity was set to 100 mW/cm^2 with a standard Si solar cell from Newport corporation.

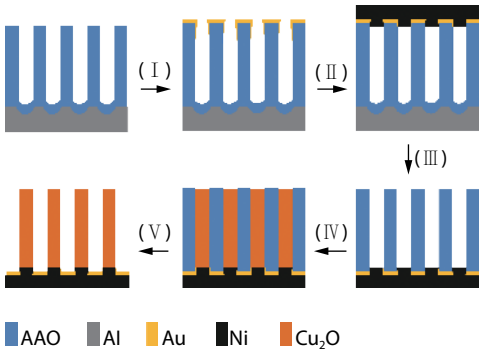

Fig. 1. (Color online) Schematic illustration of the whole fabrication procedure of Cu_2O NWs by AAO template: gold layer deposition (I), Ni electrodeposition (II), aluminum and barrier layer removal (III), Cu_2O growth (IV), and template removal (V).

2.4. Characterizations of samples

The crystal structures and mapping of the Cu_2O NWs and films were evaluated by measuring X-ray diffraction (XRD) spectra with Ni filtered Cu Kα radiation. The surface and cross-section morphologies of the samples were investigated using a scanning electron microscope (SEM, Hitachi S-570).

3. Results and discussion

The whole fabrication procedure of Cu_2O NWs can fall into 5 detailed processes that are presented schematically in Fig. 1, in which the colors of the Al, AAO, Au, Ni and Cu_2O are illustrated as gray, blue, yellow, black and orange, respectively. The process includes gold layer deposition (I), Ni electrodeposition (II), aluminum and barrier layer removal (III), Cu_2O growth (IV), and template removal (V). The AAO templates were employed as the main template during the preparation for the dramatic advantages, such as highly adjustable structural parameters, uniform and well oriented nano-porous structures, large surface area, cost-effective and good thermal stability and high mechanical strength[23–25].

Fig. 2(a) clearly illustrates that bare AAO template, which was fabricated with two times oxidization[24, 25], shows quite uniform distribution of nanopores with ~150 nm in diameter and ~5 μm in length. The Cu_2O NWs and films were prepared by anodic electrodeposition, which was in a Cu sulphate bath added 3 M 2-hydroxy propionic acid, by following the previously reported processes[15]. Fig. 2(b) shows the representative scanning electron microscopic (SEM) images of the as-grown nanowires of Cu_2O on nano-Ni substrate. And the Cu_2O nanowires are arranged vertically and neatly on the substrate. The size of the nanowires is gauged as 4.5 μm around in length and 85 nm around in diameter, respectively. The films of Cu_2O grown on the substrates of Au/FTO glass are fabricated by continuously distributed polyhedral particles, as shown in Fig. 2(c)[15]. Numerous attentions make the promotion and/or utilizations of PEC materials, especially in nanostructure to be used in splitting water ($H_2O \rightarrow \frac{1}{2} O_2 + H_2$) systems. Also involving these photocatalysts to light-absorbers, this is unique since catalysts utilization in standard electrolysis. The most noteworthy alteration is that light-coupled electrolysis needs absorbers across on large areas to raise irradiation flux capture. On the other hand, when a catalyst is straight re-

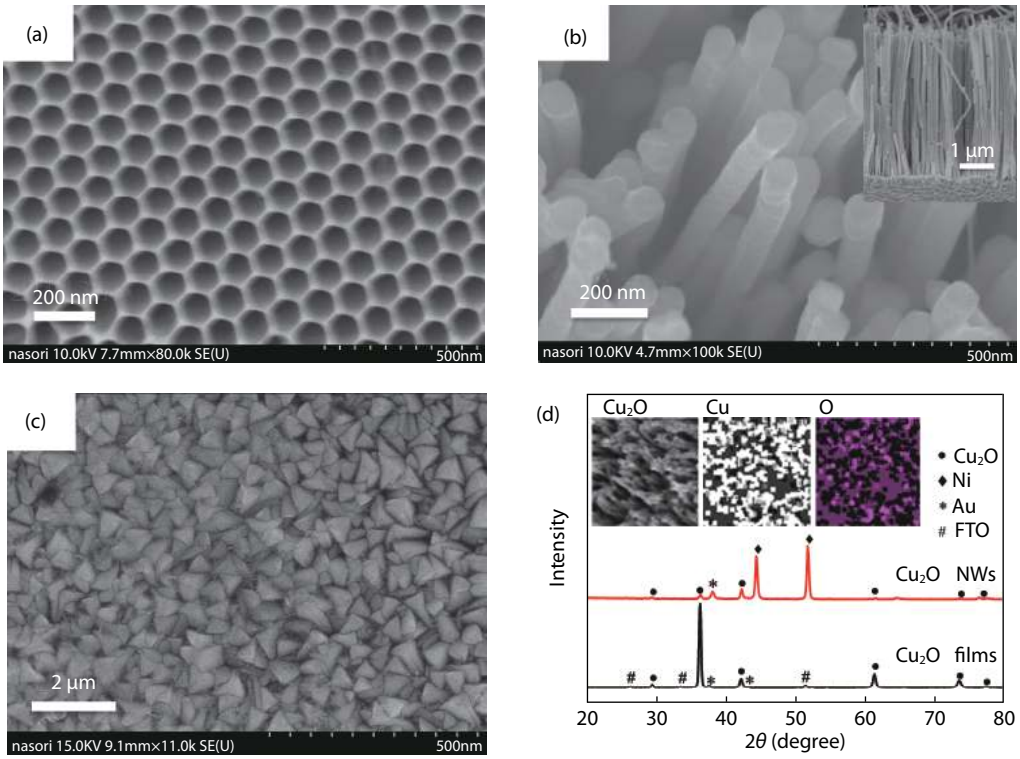

Fig. 2. (Color online) SEM images of (a) the as-prepared AAO template, (b) Cu_2O NWs (inset is cross-sectional SEM image of Cu_2O NWs) and (c) Cu_2O films. (d) The corresponding XRD patterns of Cu_2O NWs and films (inset is mapping of Cu_2O NWs).

leased on the absorber surface that will harshly inferior the requirements for current detection per unit geometric area.

In addition, the band gap of the grown films of Cu_2O is measured as 2.1 eV by the UV–vis spectrums reported in our previous paper[15], which is consistent with the reported values[22, 23].

The corresponding XRD patterns of the Cu_2O NWs and films are given in Fig. 2(d), where the diffraction peaks at 29.6°, 36.5°, 42.4°, 61.4° and 73.6° can be no doubtfully classified to the reflection of planes (110), (111), (200), (220) and (311) of the polycrystalline Cu_2O, which are consistent with the No. 05-0667 in JCPDS card[26]. Phases of Cu and CuO are not distinguishable, suggesting a pure Cu_2O structure in the nanowires and films. For further determination of the composition of the material elements, we characterized the mapping of Cu_2O NWs with SEM, as shown in inset of Fig. 2(d), which sustains that just Cu and O elements are appear in the nanowires.

Fig. 3(a) demonstrates the typical stable state EQY curves of the photoelectrodes of Cu_2O NWs and films. Comparing to Cu_2O thin films photoelectrode, the Cu_2O NWs photoelectrode on the nano-Ni exhibits an increscent EQY below the absorption threshold of Cu_2O (600 nm). An enhancement of 2-fold is obtained, indicating that Cu_2O NWs based electrode has a larger photo-to-current efficiency than that with Cu_2O thin films. This result is consistent with those reported in recent studies that have focused on the outstanding light and electric properties of nanowires and improvement in photocatalytic performance of semiconductor nanowires[27, 28].

J–V curves were characterized by immersing the PEC electrodes in 0.1 M sodium sulfate solutions, with the reference of Ag/AgCl and the counter electrode of Pt wire. Each plot represents a typical photo-response obtained under simulative light source (AM 1.5 G, 100 mW/cm^2), as illustrated in Fig. 3(b). These data reveal a cathodic photocurrent and imply a obvious p-type characteristic of both samples of Cu_2O NWs and films, which are consistent with our previous report[15]. In the system, photo-induced electrons move from films and nanowires to electrolyte to drive PEC reactions, and the corresponding holes transport from films and nanowires to ITO electrode during the PEC measurement. To be exciting, compared to the Cu_2O films electrode, the photocathode of Cu_2O NWs possesses a remarkable improvement in PEC performance, in good agreement with EQY measurement. To be noted, both Cu_2O films and NWs photoelectrode have the photoreduction peak at 0 V versus Ag/AgCl, owing to the weak chemical stabilization of Cu_2O, which is consistent with other literature reported[14].

As illustrated in Fig. 3(c), to study the PEC performance and stability under visible light of samples, the time-dependent photocurrent (*J–t*) profiles of the Cu_2O NWs and films was given with chopped light illumination (on: 250 s; off: 250 s) at –0.3 V versus Ag/AgCl. The results demonstrated that both samples exhibit photocurrent responses under each illumination quickly and reproducibly. The plateau photocurrent density of the Cu_2O films electrode was –0.11 mA/cm^2, while that of the Cu_2O NWs was –0.71 mA/cm^2, which represents a more 500% increase from the Cu_2O films. The result demonstrates that nanostructure of materials can achieve the improvement of the photoelectric conversion, owing to the capability of offering large surface area and more reaction sites, decoupling light absorption and the collection of charge carrier, shorting diffusion distance of charge carrier compared to the bulk structures[29, 30].

To elucidate the strong correlation between nanostructures and the enhanced photocurrent and EQY values, electrochemical impedance measurement was carried out. Fig. 3(d) shows Nyquist Impedance spectra of Cu_2O NWs and films at

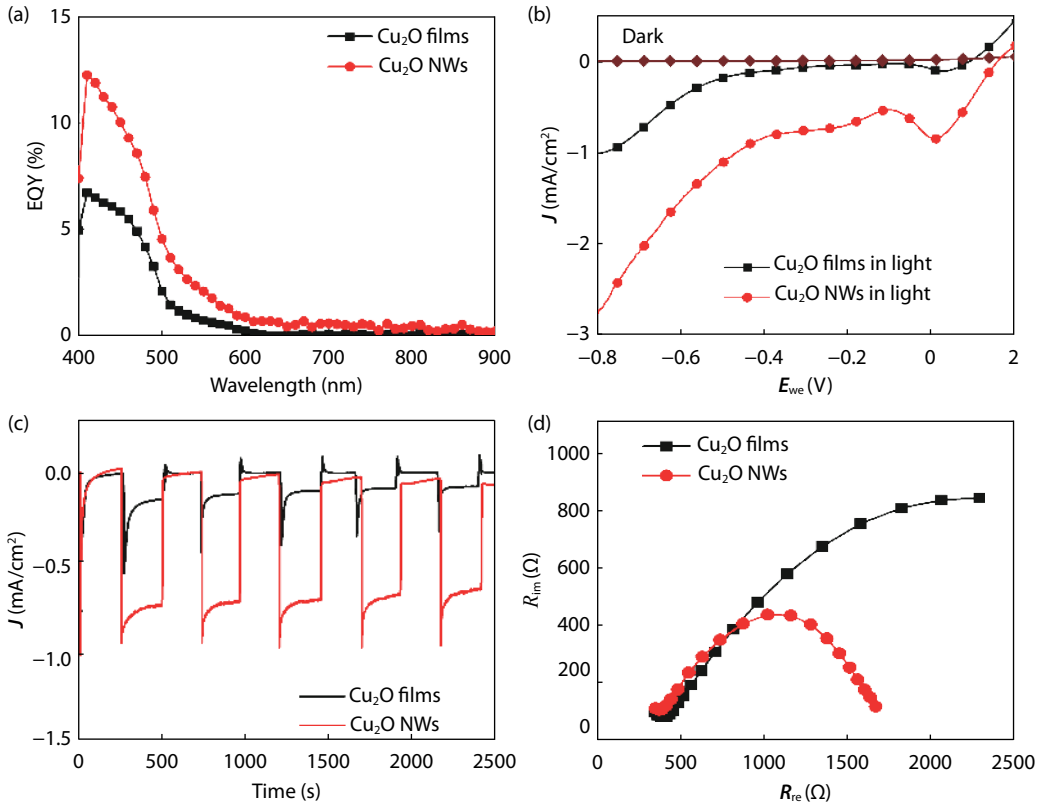

Fig. 3. (Color online) (a) EQY spectra, (b) photocurrent–potential profiles, (c) time-dependent photocurrent density spectra and (d) impedance spectra of the Cu_2O NWs and films photoelectrode.

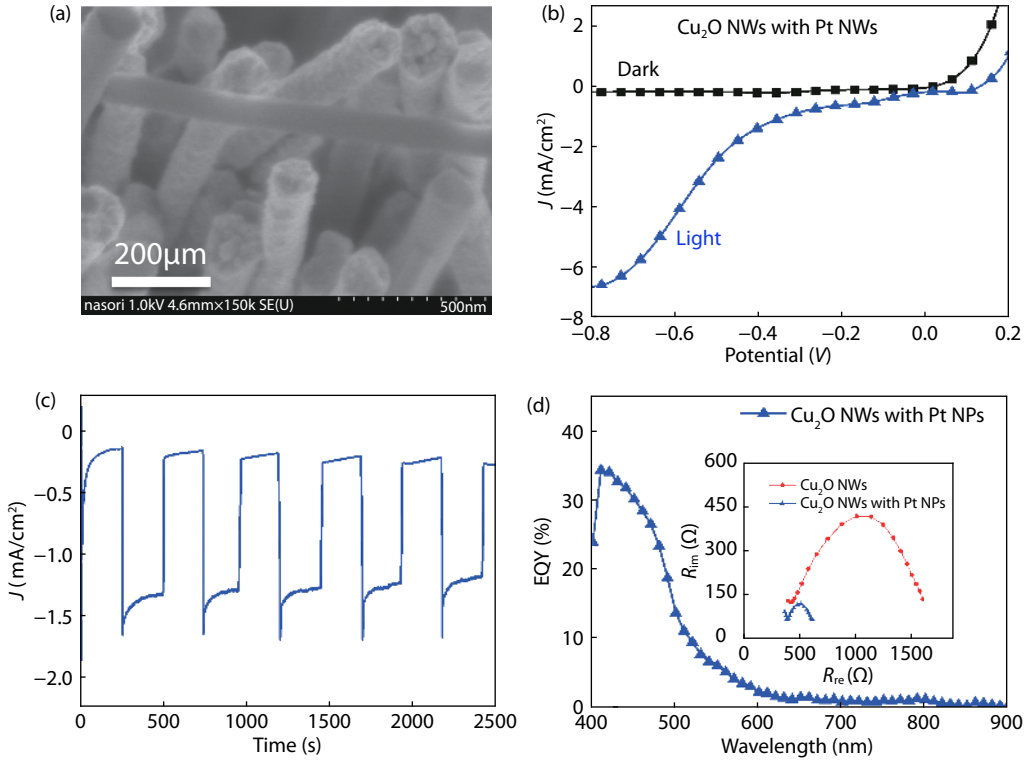

Fig. 4. (Color online) (a) Top-view SEM image of Cu_2O NWs with Pt NPs. (b) Photocurrent–potential curves and (c) photocurrent-time profile at –0.3 V versus Ag/Ag and (d) EQY spectra of the photoelectrode based on Cu_2O NWs with Pt NPs. The inset is impendence spectra.

DC frequency (200 kHz – 200 Hz) performed at open circuit voltage. In the electrolyte, Rct can be figured with fitting the semi-arc in 1 kHz region[31], which reflects the interfacial charge-transfer resistance between the working electrode and electrolyte. Smaller circular radius results in a lower resistance of electron transport and higher efficiency of separation

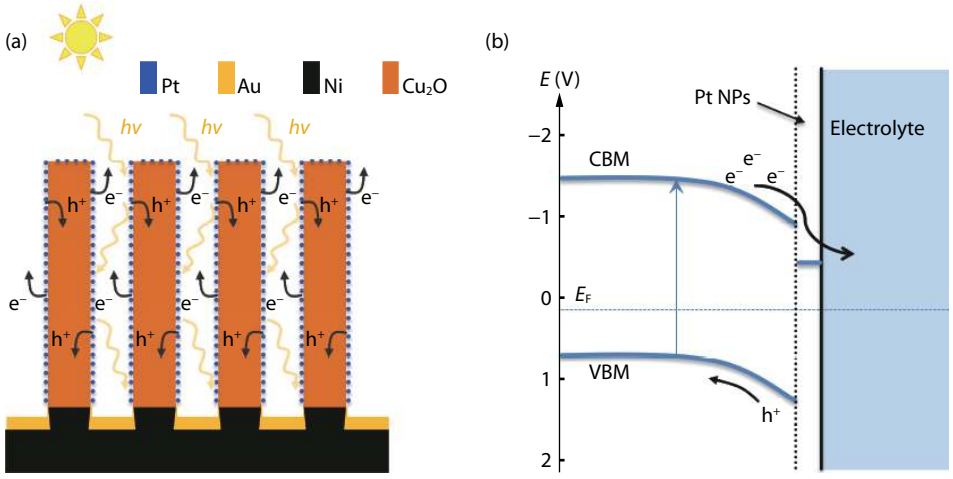

Fig. 5. (Color online) (a) Schematic diagram of Cu_2O NWs/Pt photoelectrode and (b) energy band-gap spectrum of the Cu_2O NWs with/without Pt NPs.

between photo-excited positive and negative charges. As shown in Fig. 3(d), the charge transfer resistance of Cu_2O NWs electrode is much smaller than that of Cu_2O film sample, indicating a much smaller electron transport resistance and a larger photo response, leading to a larger photocurrent in Cu_2O NWs electrode.

To further improve the performance of PEC in Cu_2O nanodevice, Pt NPs were deposited on the nanowire surrounds, which is the catalyst by a procedure of the ALD[32, 33]. Fig. 4(a) displays the top view SEM image of the catalyst on Cu_2O NWs, where the particles' size can be gauged as 5–10 nm, and Pt NPs are uniformly and high density coated on the Cu_2O NWs. The photocurrent-potential curves of the improved photocathode are shown in Fig. 4(b). By comparing with the bare Cu_2O NWs electrode, the one modified with Pt NPs catalyst has an effective enhancement in photocurrent, which is amplified to -7 mA/cm^2. Moreover, the photocurrent-time profile of the photoelectrode at –0.3 V versus Ag/AgCl (Fig. 4(c)) shows that there is no apparent decrease in current density during about 2500s time span after several light–dark period. To be surprising, by modifying the Cu_2O NWs surface with Pt NPs, the EQY is amplified to 34%, which is 2-fold of the bare Cu_2O NWs and 4-fold of Cu_2O films, which showing a great latent application of Cu_2O in water splitting, as shown in Fig. 4(c).

To shed light on the enhancement mechanism of PEC performance in Cu_2O NWs with Pt NPs, the schematic illustration of Cu_2O NWs/Pt photoelectrode and the total band energy spectrum of the Cu_2O/Pt/electrolyte structure are schematically presented in Fig. 5. The bending band of Cu_2O/Pt/electrolyte is similar to that case for p-Si/Pt/ electrolyte contact in a photoelectrochemical cell[34]. Photons absorbed by Cu_2O NWs generate minority-carriers (electrons), which drifts to the interface of photoelectrode/electrolyte where water was decomposed (from H_3O^+ to H_2). As an electrocatalyst for the photocathodic reaction (hydrogen generation), Pt NPs greatly increase the specific surface area and catalytic activity during photochemical reaction[35].

4. Conclusion

In conclusion, we have shown that a novel photocathode based on super-long Cu_2O NWs was successfully fabricated via the anodic alumina oxide template method. In comparison with the photocathode of Cu_2O films, the Cu_2O NWs photocathode demonstrates a significant enhancement in photocurrent, from –1.00 to –2.75 mA/cm^2, attributing to advantages of the nanostructure including high specific surface area, light-trapping and short carriers transfer. After optimization of the photoelectrochemical electrode through depositing Pt NPs with ALD technology on the Cu_2O NWs, the plateau of photocurrent has been enlarged to –7 mA/cm^2 furthermore. This work provides a low-cost, naturally abundant nanowire material for application in photoelectrochemical cells.

Acknowledgements

This work was supported by European Research Council (HiNaPc: 737616), European Research Council (ThreeDsurface: 240144), BMBF (ZIK-3DNanoDevice: 03Z1MN11), DFG (LE 2249_4-1), BMBF (Meta-ZIK-BioLithoMorphie: 03Z1M511), National Natural Science Foundation of China (Nos. 21577086, 51702130, 21503209), Natural Science Foundation of Jiangsu Province (BK 20170550), Jiangsu Specially-Appointed Professor Program, Hundred-Talent Program (Chinese Academy of Sciences), Beijing Natural Science Foundation (No. 2162042) and Key Research Program of Frontier Science, CAS (No. QYZDB-SSW-SLH006).

References

[1] Fujishima A, Honda K. Electrochemical photolysis of water at a semiconductor electrode. Nature, 1972, 238, 37
[2] Ni M, Leung M K H, Leung D Y C, et al. A review and recent developments in photocatalytic water-splitting using TiO_2 for hydrogen production. Renew Sustain Energy Rev, 2007, 11(3), 401
[3] Zou Z, Ye J, Sayama K, et al. Direct splitting of water under visible light irradiation with an oxide semiconductor photocatalyst. Nature, 2001, 414, 625
[4] Khan S U M, Al-Shahry M, Ingler W B. Efficient photochemical water splitting by a chemically modified n-TiO_2. Science, 2002, 297, 2243
[5] Walter M G, Warren E L, McKone J R, et al. Solar water splitting cells. Chem Rev, 2010, 110, 6446
[6] Bard A J, Fox M A. Artificial photosynthesis: solar splitting of water to hydrogen and oxygen. Acc Chem Res, 1995, 28(3), 141
[7] Kudo A, Miseki Y. Heterogeneous photocatalyst materials for wa-

ter splitting. Chem Rev, 2009, 38, 253
[8] Chen X, Shen S, Guo L, et al. Semiconductor-based photocatalytic hydrogen generation. Chem Rev, 2010, 110(11), 6503
[9] Liu R, Zheng Z, Spurgeon J, et al. Enhanced photoelectrochemical water-splitting performance of semiconductors by surface passivation layers. Energy Environ Sci, 2014, 7, 2504
[10] Moniz S J A, Shevlin S A, Martin D J, et al. Visible-light driven heterojunctionphotocatalysts for water splitting-a critical review. Energy Environ Sci, 2015, 8, 731
[11] Cao D, Wang C, Zheng F, et al. High-efficiency ferroelectric-film solar cells with an n-type Cu_2O cathode buffer layer. Nano Lett, 2012, 12(6), 2803
[12] Hara M, Kondo T, Komoda M, et al. Cu_2O as a photocatalyst for overall water splitting under visible light irradiation. Chem Commun, 1998, 3, 357
[13] Xiang C, Kimball G M, Grimm R L, et al. 820 mV open-circuit voltages from Cu_2O/CH_3CN junctions. Energy Environ Sci, 2011, 4, 1311
[14] Paracchino A, Laporte V, Sivula K, et al. Highly active oxide photocathode for photoelectrochemical water reduction. Nat Mater, 2011, 10, 456
[15] Cao D, Nasori N, Wang Z. Facile surface treatment on Cu_2O photocathodes for enhancing the photoelectrochemical response. Appl Catal B, 2016, 198, 398
[16] Ghadimkhani G, de Tacconi N R, Chanmanee W, et al. Efficient solar photoelectrosynthesis of methanol from carbon dioxide using hybrid CuO–Cu_2O semiconductor nanorod arrays. Chem Commun, 2013, 49, 1297
[17] Cao M, Hu C, Wang Y, et al. A controllable synthetic route to Cu, Cu_2O, and CuO nanotubes and nanorods. Chem Commun, 2003, 1, 1884
[18] Tan Y, Xue X, Peng Q, et al. Controllable fabrication and electrical performance of single crystalline cu_2o nanowires with high aspect ratios. Nano Lett, 2007, 7(12), 3723
[19] Zhang J, Liu J, Peng Q, et al. Nearly monodisperse Cu_2O and CuO nanospheres: preparation and applications for sensitive gas sensors. Chem Mater, 2006, 18(4), 867
[20] Ben-Shahar Y, Vinokurov K, de Paz-Simon H, et al. Photoelectrochemistry of colloidal Cu_2O nanocrystal layers: the role of interfacial chemistry. J Mater Chem A, 2017, 5, 22255
[21] Singh D P, Neti N R, Sinha A S K, et al. Growth of different nanostructures of Cu_2O (nanothreads, nanowires, and nanocubes) by simple electrolysis based oxidation of copper. J Phys Chem C, 2007, 111(4), 1638
[22] Wang Z, Cao D, Xu R, et al. Realizing ordered arrays of nanostructures: A versatile platform for converting and storing energy efficiently. Nano Energy, 2016, 19, 328
[23] Lei Y, Zhang L D, Meng G W, et al. Preparation and photoluminescence of highly ordered TiO_2 nanowire arrays. Appl Phys Lett, 2001, 78, 1125
[24] Lei Y, Cai W, Wilde G. Highly ordered nanostructures with tunable size, shape and properties: A new way to surface nano-patterning using ultra-thin alumina masks. Prog Mater Sci, 2007, 52(4), 465
[25] Lei Y, Yang S, Wu M, et al. Surface patterning using templates: concept, properties and device applications. Chem Soc Rev, 2011, 40, 1247
[26] Azimi H, Kuhri S, Osvet A, et al. Effective ligand passivation of Cu_2O nanoparticles through solid-state treatment with mercaptopropionic acid. J Am Chem Soc, 2014, 136(20), 7233
[27] Law M, Greene L E, Johnson J C, et al. Nanowire dye-sensitized solar cells. Nat Mater, 2005, 4, 455
[28] Pauzauskie P J, Yang P. Nanowire photonics. Mater Today, 2006, 9(10), 36
[29] Sun H, Deng J, Qiu L, et al. Recent progress in solar cells based on one-dimensional nanomaterials. Energy Environ Sci, 2015, 8, 1139-1159
[30] Zhang Q, Cao G. Nanostructured photoelectrodes for dye-sensitized solar cells. Nano Today, 2011, 6(1), 91
[31] Zheng F G, Zhang P, Wang X F, et al. Photovoltaic enhancement due to surface-plasmon assisted visible-light absorption at the inartificial surface of lead zirconate-titanate film. Nanoscale, 2014, 6(5), 2915
[32] Ibhadon A, Fitzpatrick P. Heterogeneous photocatalysis: recent advances and applications. Catalysts, 2013, 3(1), 189-218
[33] Kamat P V. Graphene-based nanoarchitectures anchoring semiconductor and metal nanoparticles on a two-dimensional carbon support. J Phys Chem Lett, 2010, 1(2), 520
[34] Oh I, Kye J, Hwang S. Enhanced photoelectrochemical hydrogen production from silicon nanowire array photocathode. Nano Lett, 2012, 12(1), 298
[35] Kinoshita K. Carbon: electrochemical and physicochemical proper. New York: John Wiley Sons, 1988